# A Membrane Anchored DNA Assembly for Energy and Electron Transfer

*Karl Börjesson,† John Tumpane,† Thomas Ljungdahl,† L. Marcus Wilhelmsson,† Bengt Nordén,† Tom Brown,‡ Jerker Mårtensson† and Bo Albinsson†**

†Department of Chemical and Biological Engineering, Chalmers University of Technology, SE-41296 Gothenburg, Sweden

‡School of Chemistry, University of Southampton, Highfield, Southampton, SO17 1BJ, UK

Email: balb@chalmers.se

Telephone: +46-(0)31-7723044

Fax: +46-(0)31-7723858

**Abstract:** In this work we examine the trapping and conversion of visible light energy into chemical energy using a supramolecular assembly. The assembly consists of a light-absorbing antenna and a porphyrin redox centre which are covalently attached to two complementary 14-mer DNA strands, hybridized to form a double helix and anchored to a lipid membrane. The excitation energy is finally trapped in the lipid phase of the membrane as a benzoquinone radical anion that could potentially be used in subsequent chemical reactions. In addition, in this model complex the hydrophobic porphyrin moiety acts as an anchor into the liposome positioning the DNA construct on the lipid membrane surface. The results show the suitability of our system as a prototype for DNA based light-harvesting devices, in which energy transfer from the aqueous phase to the interior of the lipid membrane is followed by charge separation.

## Introduction

Mimicking nature's photosynthetic machinery has been a long-standing scientific goal for many research groups. Artificial photosynthesis has today developed into an art that has constructed light harvesting antennae, electron transfer reaction centers, and combinations of the two but we are still quite far from the final goal.[1-3] A limiting factor is the rate at which synthesis of new assemblies can be made, since traditional organic synthesis is inherently slow for complicated multi-component systems of the kind encountered in this field. It is therefore tempting to make use of the controlled self-assembly of nucleic acids to construct ordered arrays of chromophores and redox centers.

Lipid membranes are exceptionally useful substrates on which to anchor light-harvesting chromophores since they allow for ease of self-assembly and relatively fast diffusion in two dimensions across the surface. Moreover, they provide an excellent bridge between the aqueous phase and any potential surface on which the bilayer is deposited.[4-6] The supramolecular system investigated in this work consists of a short DNA oligonucleotide (14 base pairs) to which a hydrophobic porphyrin has been covalently attached (oligo-ZnP), and this in turn is incorporated into a lipid membrane.

Hybridization with a complementary DNA strand having fluorophores (fluorescein, FAM) attached at either of the two ends gives rise to a supramolecular system capable of sequential energy and electron transfer reactions. The complete assembled system is schematically depicted in Figure 1. The porphyrin is a multi-functional component that can act as an electron- and/or energy transfer component, an anchor to the surface and a ligand docking site for potential co-ordination interactions. By exploiting the lipophilicity of the porphyrin functionality the oligonucleotide can be bound to large unilamellar lipid vesicles (liposomes, approximately 100 nm in diameter). This positions the porphyrin chromophore in the hydrophobic environment of the membrane and the hydrophilic DNA part of the system at the interface, but still in the water phase. Preferential localization of hydrophobic molecules in the membrane ensures that the concentration of solutes, *e.g.* electron acceptors, typically organic molecules, can be held quite high without disrupting the DNA "antenna" in the water phase. The use of liposomes to support energy and electron transfer systems has previously been used by Clapp *et al.* who used negatively charged lipids to bind positively charged chromophores at such high concentrations that energy transfer becomes efficient.[7] Also the use of liposomes to solubilize zinc porphyrins has previously been demonstrated.[8-10] Recently a DNA-porphyrin system based on a very similar modified nucleotide was used to examine the potential of a DNA duplex as a molecular scaffold.[11]

The DNA molecule has come to the fore in recent years as an excellent building-block for dynamic yet robust nanotechnological applications. In previous work we demonstrated the construction of addressable nanometer scale DNA nanostructures based on a hexagonal unit cell where energy transfer can be targeted at specific locations.[12, 13] Networks based on such addressability have the potential to offer spatial resolution of subnanometer precision. The incorporation of functionalities into such a system with very precise knowledge of location could be the basis of useful applications. In this work the usefulness of a zinc porphyrin (ZnP) functionality covalently attached to a DNA strand is examined. Porphyrins are very versatile molecules that can be fine-tuned by the use of different co-ordinated metal ions and act as models for light-harvesting systems. The molar absorptivity of the zinc porphyrin is high

($\varepsilon$ = 20000 $M^{-1}$ $cm^{-1}$ at 544 nm) and in a wavelength range where many common fluorophores emit light, *e.g.* fluorescein (FAM) and rhodamine (Rhodamine 110), making the zinc porphyrin a suitable excitation energy acceptor. Thus, if a zinc porphyrin energy sink is combined with an addressable two-dimensional network a supramolecular nanoscale light-harvesting system is created where energy collected by the DNA array can be transferred to the supporting liquid crystalline phase. Our model system consists of a 14-mer oligonucleotide where one thymidine nucleotide is replaced by a modified one to which a zinc porphyrin is covalently attached via a linker at the 5-position of the thymine base. The linker consists of a rigid phenylacetylene moiety and is designed so that the porphyrin protrudes from the DNA through the major groove. The porphyrin-dT is placed five nucleotides from the 5′ terminus, and by hybridizing the porphyrin DNA strand to a complementary strand containing a fluorescein on either the 5′ or 3′ end, two systems with different chromophore-chromophore distance are created (separated by 9 or 4 base pairs). These two systems have been used to probe the efficiency of energy transfer from the DNA to the bilayer-bound porphyrin moiety. Furthermore, the electron transfer characteristics have been investigated using 2,6-di-*t*-butyl-*p*-benzoquinone (BQ) as an acceptor and the co-ordination addressability has been studied using 4-*t*-butylpyridine (tBP) as a ligand, again in the membrane. The results in both cases indicate the suitability of our chosen system as a prototype for DNA-based light-harvesting devices, with energy subsequently transferred to organic molecules in a lipid bilayer.

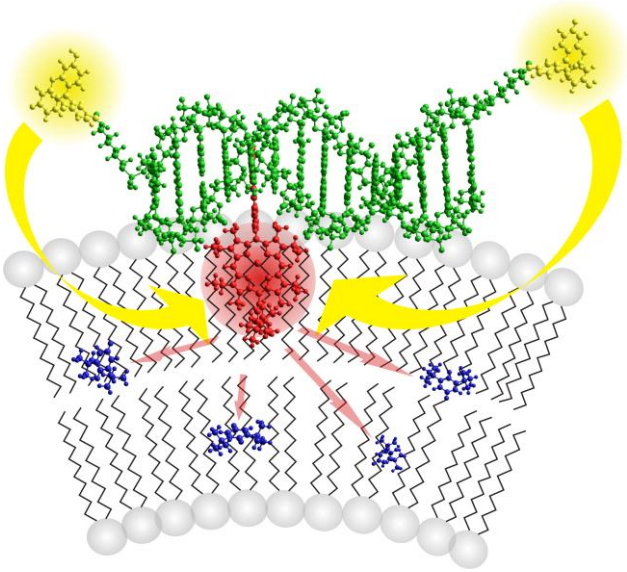

**Figure 1.** Schematic picture of the supramolecular system. The DNA shown in green is attached covalently to a hydrophobic porphyrin (red). A fluorescein is also attached covalently on one of the two ends on the complementary DNA strand. Energy transfer from the fluorescein to the zinc porphyrin is illustrated and electron transfer to hydrophobic 2,6-di-*t*-butyl-*p*-benzoquinone (blue) in the membrane is also depicted.

## Materials and Methods

### *Synthesis*

Commercially available reagents were used without further purification. The DMT protected deoxyuridine, 5′-dimethoxytrityl-5-iodo-2′-deoxyuridine, was prepared according to a literature procedure in near quantitative yield and the spectroscopic data were in accordance with that published.[14] The synthesis of the porphyrin starting material **1** (Scheme 1) is described elsewhere.[15]

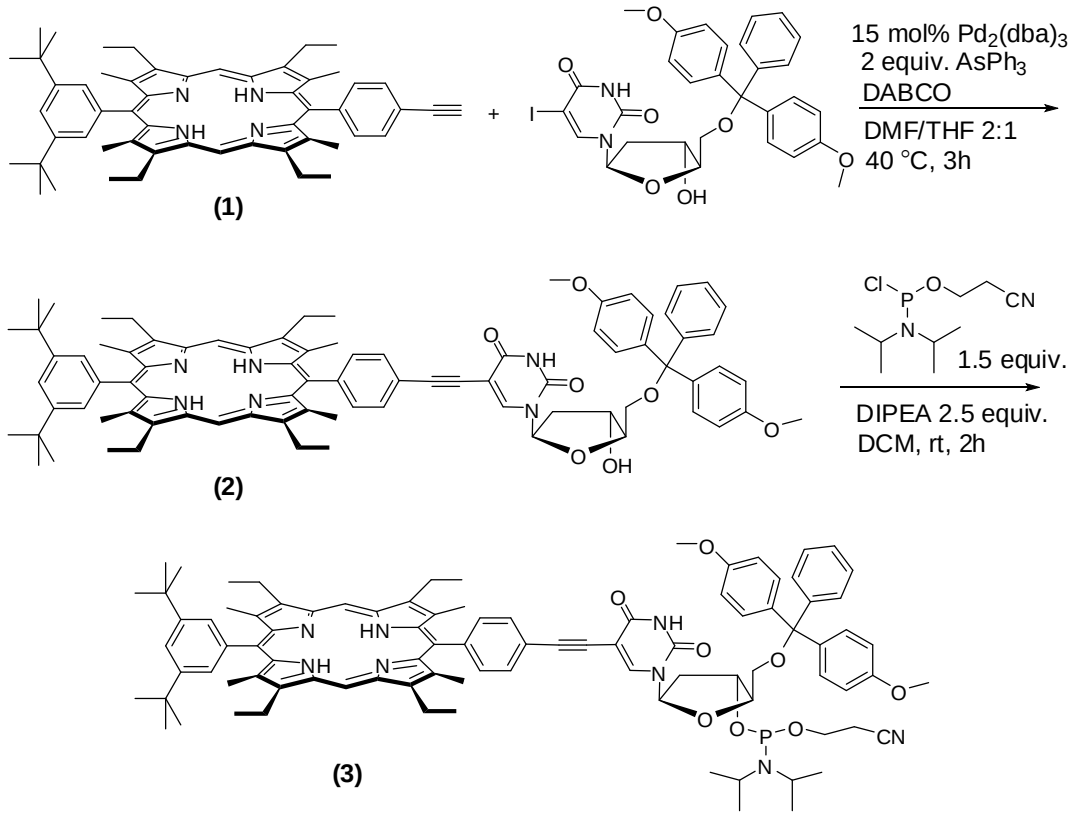


**Scheme 1.** The synthesis of the porphyrin dT monomer by copper-free Sonogashira cross-coupling and phosphoramidation.

De-oxygenation of reaction mixtures was achieved by bubbling argon through the solution for 30 minutes. Palladium-catalyzed reactions were performed under argon and protected from light by aluminium foil. Column chromatography and flash chromatography were generally performed using silica gel (Matrex, LC 60 Å / 35–70 μm). Chromatography of porphyrins was performed using silica gel (Merck, grade 60, 230–400 mesh). Size exclusion chromatography (SEC) was performed on BioRad Bio-Beads SX–3 in PhCl/DMF 2:1. $^{1}$H (400 MHz) and $^{13}$C (100.6 MHz) NMR spectra were recorded at room temp. in $CDCl_3$ using a Jeol Eclipse 400 NMR spectrometer. Chemical shifts are reported relative to residual $CHCl_3$ ($\delta$ = 7.26 ppm) for $^{1}$H NMR and $CDCl_3$ ($\delta$ = 77.23 ppm) for $^{13}$C NMR. All coupling constants given are for (H,H) couplings. Positive FAB high resolution mass spectra were obtained on a JEOL SX102 mass spectrometer at Instrumentstationen, Lund University, Sweden. Samples were desorbed from a 3-NBA matrix using 6 kV xenon atoms.

**2**: $Pd_2(dba)_3$•$CHCl_3$ (10.1 mg, 9.8 μmol) was added to a degassed solution of **1** (50 mg, 0.065 mmol), 5′-dimethoxytrityl-5-iodo-2′-deoxyuridine (64 mg, 0.098 mmol), $AsPh_3$ (24.0 mg, 0.078 mmol) and DABCO (146 mg, 1.30 mmol) in DMF/THF (3:2, 5 mL). The reaction mixture was stirred for 2 h at 40°C followed by removal of the solvent in vacuo. Rough chromatography ($SiO_2$, $CH_2Cl_2$ → 2% MeOH in $CH_2Cl_2$) followed by SEC (chlorobenzene/DMF, 2:1) gave **2** as a red solid (69.3 mg, 0.054 mmol, 83%); $^1$H NMR ($CDCl_3$) δ = -2.46 (br s, 2H), 1.50 (s, 18H), 1.76 (m, 12H), 2.13 (m, 1H), 2.44 (s, 6H), 2.46 (s, 6H), 2.58 (m, 1H), 3.40 (m, 1H), 3.60 (m, 1H), 3.79 (s, 6H), 4.03 (m, 8H), 4.17 (m, 1H), 4.63 (br m, 1H), 6.45 (m, 1H), 6.91 (m, 4H), 7.24-7.48 (m, 9H), 7.55 (d, $^3$J = 8Hz, 2H), 7.82 (t, $^4$J = 2 Hz, 1H), 7.89 (d, $^3$J = 8 Hz, 2H), 7.92 (d, $^4$J = 2 Hz, 2H), 8.41 (s, 1H), 8.51 (br s, 1H), 10.24 (s, 2H) ppm; HRMS (FAB+) calcd. for [$C_{84}H_{91}N_6O_7$]: 1295.6949, found: 1295.6954

**3:** The DMT-protected porphyrin nucleoside **2** (105 mg, 0.081 mmol) was dissolved in 3 mL of thoroughly degassed dichloromethane. 2-Cyanoethyl N,N-diisopropylchlorophosphoramidite (29 mg, 0.121 mmol, 27 μL) and diisopropylethylamine (26 mg, 0.203 mmol, 35 μL) was added via cannula. After two hours the product was dissolved in 20 ml of degassed dichloromethane and washed twice with aqueous KCl. The solvent was evaporated and the crude mixture dissolved in 3 ml EtOAc/hexane 7:3. Chromatography ($SiO_2$, EtOAc/hexane 7:3) under nitrogen gave the red solid product as a mixture of two diastereomers (62.5 mg, 0.042 mmol, 52%). The incorporation of phosphorus was confirmed by $^{31}$P NMR spectroscopy but no further characterization or purification was performed on the very air sensitive phosporamidite product. It was immediately loaded into the solid phase synthesizer; $^{31}$P NMR ($CDCl_3$) δ = 148.88, 148.57 ppm.

***Oligonucleotide synthesis***

Standard and modified Deoxyribonucleoside phosphoramidite monomers, solid supports and additional reagents for oligonucleotide synthesis were purchased from Link Technologies Ltd (Glasgow UK) and Applied Biosystems Ltd (Warrington UK). All oligonucleotides were synthesized on an Applied Biosystems 394 automated DNA/RNA synthesizer using a standard 1.0 μmole phosphoramidite

cycle of acid-catalyzed detritylation, coupling, capping, and iodine oxidation. Standard A, G, C and T monomers were coupled for 35 sec and labeling monomers (FAM, BHQ-1 and porphyrin) were coupled for 6 min. Stepwise coupling efficiencies and overall yields were determined by the automated trityl cation conductivity monitoring facility and in all cases were >98.0%. Cleavage of oligonucleotides from the solid support and deprotection were achieved by exposure to concentrated aqueous ammonia solution for 60 min. at room temperature followed by heating in a sealed tube for 5 h at 55°C. Zinc insertion was accomplished by means of treating the free-base oligonucleotide with $Zn(OAc)_2 \bullet H_2O$ (1% w/w in MeOH) at 70°C for 5 minutes. At high oligo concentrations the addition of zinc acetate sometimes caused precipitation. However, the oligos redissolved by the addition of a few drops of aqueous ammonia (5% in $H_2O$). The oligonucleotides were purified by gel-filtration on a NAP-10 column (GE Healthcare) according to the manufacturer's instructions. To check the insertion of the porphyrin nucleoside MALDI-TOF (matrix-assisted laser desorption ionization time-of-flight, positive mode) was performed on a test sequence consisting of 12 dT where one dT was substituted by the porphyrin-dT. The check was performed on both the free-base 12 dT-oligonucleotide and its zinc analogue. No trace of the free-base 12 dT-oligonucleotide could be detected in the spectrum of the metallated analogue, indicating that complete metallation was taking place. (calc. 12 dT oligo-$H_2$P [$C_{173}H_{216}N_{28}O_{82}P_{11}$] 4339.07, found 4339.4; calc. 12 dT oligo-ZnP [$C_{173}H_{214}N_{28}O_{82}P_{11}Zn$] 4400.99 found 4401.5).

***Liposome preparation***

1,2-Dioleoyl-*sn*-glycero-3-phosphocholine (DOPC) was purchased from Larodan. Large unilamellar vesicles (LUVs) were prepared by standard procedure as briefly described here. A thin lipid film was created by evaporating a chloroform solution of the lipids, which was subsequently dissolved in aqueous buffer and subjected to freeze-thaw cycling (5 times). The solution was then extruded 21 times through 100 nm polycarbonate filters (Whatman).

***Photophysical measurements***

All measurements were made in a phosphate buffer at pH 8 in a total sodium ion concentration of 200 mM, unless otherwise stated. Oligo-ZnP and lipid concentrations were 2 μM and 200 μM, respectively, unless otherwise stated. Absorption spectra were measured on a Varian Cary 4000 spectrophotometer or on a Varian Cary 4B spectrophotometer.

**Concentration determination:** The concentrations of the oligonucleotides were determined by UV absorption measurements at 260 nm. The extinction coefficients for the oligonucleotides were calculated using a linear combination of the extinction coefficients of the nucleotides, the zinc porphyrin nucleotide and fluorescein at 260 nm. To account for the base stacking interactions, this linear combination was multiplied by 0.9 to compensate for the hypochromicity to give a final estimate of the extinction coefficients for the oligonucleotides. The individual extinction coefficients at 260 nm used in the calculation were $\varepsilon_T$ = 9300 $M^{-1}$ $cm^{-1}$, $\varepsilon_C$ = 7400 $M^{-1}$ $cm^{-1}$, $\varepsilon_G$ = 11 800 $M^{-1}$ $cm^{-1}$, $\varepsilon_A$ = 15 300 $M^{-1}$ $cm^{-1}$,[16] $\varepsilon_{fluorescein}$ = 21 000 $M^{-1}$ $cm^{-1}$ and $\varepsilon_{ZnP}$ = 32 000 $M^{-1}$ $cm^{-1}$. The sequence of oligo-ZnP was 5′-TCCGT*CTGCAGCGT-3′, where T* was the modified nucleotide.

**Dynamic light-scattering (DLS)** was used to confirm the size (radius ~ 50 nm) and monodispersity (polydispersity index ~ 0.1) of the liposomes in the solution both before and after addition of oligo-ZnP. Measurements were performed on an ALV CGS-8F DLS/SLS-5022F instrument equipped with an ALV-6010/160 correlator and dual APD detectors at a wavelength of 638.2 nm and a scattering angle of 90°. The temperature was set to 20°C with a lipid concentration of 25 μM.

**Circular Dichroism (CD)** spectra were recorded on a Jasco J-810 spectropolarimeter at 20ºC, first on the oligo-ZnP alone (2 μM) then directly upon addition of the liposomes (200 μM) and, finally, after 12 hours.

**Linear Dichroism (LD)** is a powerful technique used to infer conformational and geometric information for a given molecule. It is based on the principle that impingent light that is polarized in the same direction as the electronic transition moment will be preferentially absorbed. In order to ascertain such information it is necessary to orient the molecules with respect to the incident light. Flow linear

dichroism uses shear flow to achieve this and it has been well established that liposomes can be oriented due to their ellipsoidal deformation in such a flow.[17] By measuring the difference in absorption, $A$, between two mutually perpendicular planes of linearly polarized light structural information can be obtained if the directions of the transition moments in the molecule are known. Linear dichroism (LD) is therefore defined as:

$$LD = A_{\parallel} - A_{\perp} \qquad (1)$$

where $A_{||}$ and $A_{\perp}$ is the absorption of light polarized parallel and perpendicular to the flow, respectively. A more useful concept is the reduced linear dichroism ($LD^R$) which is the $LD$ spectrum divided by the corresponding isotropic absorption spectrum, and therefore being independent of concentration. For a uniaxially oriented system the $LD^R$ of a single electronic transition, $i$, is related to the angle $\alpha_i$ between that transition moment and the macroscopic orientation axis (the direction of the flow in this case).

$$LD_i^R = \frac{A_{\parallel} - A_{\perp}}{A_{iso}} = \frac{3}{2} S(3\cos^2 \alpha_i - 1) \qquad (2)$$

where $S$ is an orientation parameter, which is 1 for perfectly ordered systems and 0 for isotropic systems.

LD spectra were recorded on a modified Jasco J-720 CD spectropolarimeter fitted with an Oxley prism to produce linearly polarized light. A Couette cell was used to induce shear flow orientation of the samples. Measurements were performed in 50% w/w sucrose of the same phosphate buffer solution at a lipid concentration of 200 μM. The sucrose fulfils two roles, firstly refractive index matching of the liposomes to the solution greatly reduces detection problems caused by scattering and secondly the increased viscosity provides for better alignment of the liposomes.[17] The background at zero shear rate was used as a baseline for the spectra taken at a shear gradient of 3100 $s^{-1}$. Isotropic absorption measurements were made on the same samples to calculate the $LD^R$ spectrum.

**Absorbance titration:** The binding constant of the ligand, 4-*t*-butylpyridine (tBP), to oligo-ZnP in

liposomes was determined by spectrophotometric titration. The titration was performed by adding aliquots of a 2.5 mM solution of the ligand to the solution of oligo-ZnP and liposomes. A correction for the volume change was made in the subsequent analysis. In the analysis, it is assumed that the equilibrium concentration of the ligand, $c_L$, remains in large excess, so that the concentration is unchanged from that initially added, $c_{L0}$, at all points in the titration. The model used was:

$$K = \frac{c_{PL}}{c_P c_L} \approx \frac{c_{PL}}{c_P c_{L0}} \quad (3)$$

where $c_P$ is the concentration of unbound oligo-ZnP and $c_{PL}$ is the concentration of ligand bound oligo-ZnP. The set of titration spectra were analyzed at one wavelength (413.5 nm) as well as with Singular Value Decomposition (SVD). The SVD analysis was performed with an in-house made MATLAB program based on the method described in reference [18]. Briefly, the SVD method decomposes the set of titration spectra, $A$, into three matrices:

$$A = USV^T \quad (4)$$

where $U$ contains the orthogonal basis spectra, $S$ is a diagonal matrix that contains the singular values and $V$ contains the coefficient vectors. The matrixes $U$ and $V$ are pseudo-rotated into the physically meaningful spectra ($\varepsilon$) and concentration ($C$) matrixes, respectively, by requiring that the concentrations throughout the titration are related by the equilibrium constant (Eq. 3).

**Double-stranded oligonucleotides** for energy transfer experiment were formed by mixing the oligo-ZnP and the complementary strand (with fluorescein on either the 5′ or 3′ end) in phosphate buffer at room temperature yielding a double strand concentration of 1 μM (an excess of 50% of the oligo-ZnP strand was used). The samples were heated to 85°C and thereafter annealed by slowly cooling to 5°C after which the liposomes were added. The sample was then left at 5°C overnight.

**Steady state fluorescence** was measured on a Spex Fluorolog 3 spectrofluorimeter (JY Horiba), which was equipped with Glan polarizers at both the excitation and emission light paths for the anisotropy measurements.

*Fluorescence excitation anisotropy:* If a population of molecules is excited with linearly polarized light a non-randomly-oriented excited population is obtained. Subsequent fluorescence from the same transition moment will therefore have the same polarization - provided the fluorophore does not undergo rotational relaxation during the excited state lifetime. The anisotropy, *r*, is defined as the difference in fluorescence intensity (*I*) between two mutually perpendicular planes of polarization divided by the total intensity.

$$r = \frac{I_{\parallel} - I_{\perp}}{I_{\parallel} + 2I_{\perp}} \qquad (5)$$

Anisotropy can therefore be seen as a measure of the change in polarization from the absorption to the emission state over the lifetime of emission. The fundamental anisotropy, $r_0$, is the maximum anisotropy value for a certain transition, *i.e.* the anisotropy in the absence of rotation, and is given by

$$r_0 = \frac{2}{5}\left(\frac{3\cos^2\beta - 1}{2}\right) \qquad (6)$$

where $\beta$ is the angle between the excited transition moment and the transition from which emission occurs. For perfectly co-linear and for perpendicular transition moments the fundamental anisotropies are 0.4 and -0.2, respectively. In-plane degenerate transitions will have a lower apparent anisotropy, with an upper maximum at 0.1.

Fluorescence excitation anisotropy spectra were recorded from 290 to 600 nm and the emission wavelength fixed at 635 nm. Anisotropy values were calculated as the average value over a short wavelength interval corresponding to a peak in the absorption spectrum. A similar measurement was made on oligo-ZnP alone in a 1:1 methanol/ethanol glass at 77 K using an Optistat$^{DN}$cryostat (Oxford Instruments), to obtain the fundamental anisotropies.

*Steady state fluorescence quenching:* The integrated emission spectra were recorded from 558 to 750 nm and the excitation wavelength fixed at 543 nm or 495 nm when exciting zinc porphyrin or fluorescein, respectively. 2,6-di-*t*-butyl-*p*-benzoquinone (BQ) was used as a quencher. Aliquots of a BQ

stock solution were added and correction for the volume change was made in the subsequent analysis.

*Quantum yield* (QY) of the fluorescein label on DNA in buffer was measured relative to fluorescein in 0.1 M NaOH (aq) (QY=0.92) .[19]

*Fluorescence melting:* Melting curves were measured on a Varian Eclipse spectrofluorimeter equipped with a programmable multi-cell temperature block. The temperature was cycled between 10 and 55°C at 0.3°C/min. The samples were excited at 470 nm and the emission was monitored at 520 nm.

**Fluorescence lifetimes** were determined using time-correlated single photon counting. The excitation pulse was provided by a Tsunami Ti:Sapphire laser (Spectra-Physics) which was pumped by a Millenia Pro X (Spectra-Physics). The Tsunami output was modulated in an optical parametric oscillator (KTP-OPO, GWU) and acousto-optically pulse-picked to 4 MHz by a pulse selector (Spectra Physics) when needed and subsequently frequency-doubled. The photons were collected by a thermoelectrically cooled micro channel-plate photomultiplier tube (MCP-PMT R3809U-50; Hamamatsu) and fed into a multi-channel analyzer with 4096 channels. A minimum of 10000 counts were recorded in the top channel. The fluorescence decay curves were fitted to double-exponential expressions by the program FluoFit Pro v.4 (PicoQuant GMBA), individually as well as with global parameters. Oligo-ZnP in liposomes was excited at 545 nm with a laser repetition rate of 80 MHz which, because of the short lifetimes, is an appropriate frequency. The sample response was recorded through a 600 nm low pass filter to reject scattered light and monitored through a monochromator at 640±16 nm. Fluorescein was excited at 470 nm with 4 MHz at 10°C. The sample response was recorded through a polarizer at magic angle and monitored at 520±16 nm.

**Analysis of octanol/buffer partitioning:** A small amount of BQ or tBP was added to an Eppendorf tube containing equal amounts of octanol and buffer. The samples were then vortexed for 30 min. and left to separate into two phases. The concentration of solute in each phase was determined by absorption spectroscopy. To obtain equivalent solvent conditions, buffer and methanol were added to aliquots of the octanol phase and octanol and methanol were added to aliquots of the water phase. The final mixture

of buffer: octanol: methanol was 2:2:5.

## Results and Discussion

### *Synthesis*

The oligo-ZnP oligonucleotide was synthesized from protected and activated nucleoside **3** (*Scheme 1*) using solid phase synthesis techniques. The porphyrin-labelled nucleoside **3** was constructed by a copper-free Sonogashira cross-coupling reaction between the ethynyl functionalized porphyrin building block **1** and 5′-dimethoxytrityl-5-iodo-2′-deoxyuridine, followed by a conversion to the phosphoramidite monomer.

The unprotected porphyrin nucleoside was also prepared, but it was impossible to dissolve it in the concentrations required for an efficient tritylation, so this was not a viable synthetic route. Zinc was inserted after oligonucleotide synthesis. The reason for this post-synthetic metallation was twofold; the metallated phosphoramidite monomer was prone to aggregation which complicated its purification and the porphyrin would have been demetallated during the acidic conditions of the detritylation steps in solid-phase synthesis. Interestingly, the porphyrin was demetallated in deionized water which is slightly acidic, so freeze drying of the samples were performed after addition of a drop of triethylamine and all measurements were performed in basic buffer.

The conditions used for the coupling were selected from a previously published screening of different catalyst–solvent–base combinations in copper-free Sonogashira cross-couplings.[20] We deliberately avoided the use of Cu(I) given the undesired and facile metallation of porphyrins by copper.[21] The conditions selected were a catalyst system consisting of $Pd_2(dba)_3$•$CHCl_3$/$AsPh_3$/DMF/DABCO with THF as co-solvent. This produced high yields of the porphyrin nucleoside (82%) in only three hours reaction time. A coupling involving porphyrin substrates and 5-iodo-2′-deoxyuridine has previously been published and the authors reported similar yields but with reaction times as long as 48 hours using a $Pd(PPh_3)_4$/$Et_3N$/CuI/DMF catalyst system.[22] Consequently, despite the absence of copper, our conditions held up nicely in comparison to more standard Sonogashira approaches using cuprous iodide.

***Photophysical measurements***

The absorption spectrum for oligo-ZnP in Figure 2 shows several distinctive peaks, one for the DNA bases centered at 260 nm, a typical zinc porphyrin Soret band at 414 nm and the Q-band peaks at 540 and 570 nm. There is another peak at 310 nm which we attribute to a transition localized on the conjugated linker from the modified thymine base to the porphyrin functionality; justification for this will become apparent from the polarized spectroscopy measurements. The Soret band is not entirely symmetric and broader than expected from comparison to spectra in less polar solvents. The broadening can be seen in single- as well as double- stranded DNA. Addition of liposomes causes the Soret band to become much sharper and more Gaussian in form. This indicates that in free solution, there is an interaction between the porphyrin group and some other moiety. Fluorescence measurements show comparatively low luminescence from the oligo-ZnP molecule in aqueous solution, although when bound to the lipid membrane the fluorescence increases. It is likely that the same fluorescence quenching process also causes the broadening of the absorption spectrum. Probably the oligo-ZnP molecules, with the hydrophobic porphyrin group, aggregate in aqueous solutions. Similar observations have recently been reported by Fendt et al.[23]

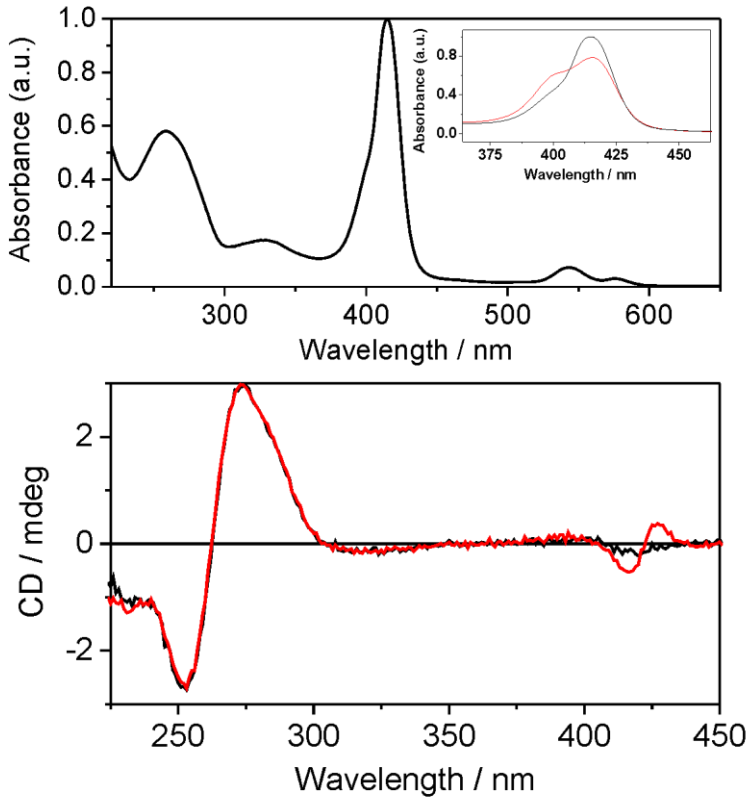


**Figure 2.** Top: Absorption spectrum of oligo-ZnP when bound to DOPC liposomes (black line) and free oligo-ZnP in aqueous solution (inset, red line). Below: Circular dichroism (CD) spectra for oligo-ZnP alone (red line) and when it is bound to liposomes (black line).

**Circular Dichroism:** A CD signal can arise from a chiral molecule with each enantiomer having a signal of different sign. The presence of a non-absorbing chiral moiety can induce a, usually much weaker, CD signal in a non-chiral molecule. Since the porphyrin group is linked to the chiral deoxyribose sugar this is a distinct possibility. Alternatively a CD signal may also be produced due to exciton coupling, where the transition moments of two distinct molecules/moieties interact over short distances. The CD spectrum in Figure 2 shows a clear and reasonably strong bisignate peak for the zinc porphyrin Soret band of oligo-ZnP in free solution as well as a typical single stranded DNA signal at shorter wavelengths. Upon addition of liposomes the intensity of the Soret band CD immediately decreases until eventually disappearing. This is clear evidence that the Soret band CD is caused by

exciton coupling due to hydrophobic stacking of the porphyrin groups and not an induced CD due to the chiral DNA and that the stacking of oligo-ZnP does not appear to take place in the bilayer. In order for the aggregates to exhibit an excitonic CD the aggregates must have a preferred helicity which in this case is imposed by the presence of the bulky DNA single strands. The aggregates must therefore be broken up by addition of the liposomes, indicating a near quantitative membrane localization of the porphyrin and hence DNA at the bilayer/interface. There may be a very slight residual CD due to a small amount not being bound or to a weak induced CD from the chiral sugar. The other peaks in the zinc porphyrin absorption do not give rise to any measurable CD signal which is not unexpected since they have much lower molar absorptivities.

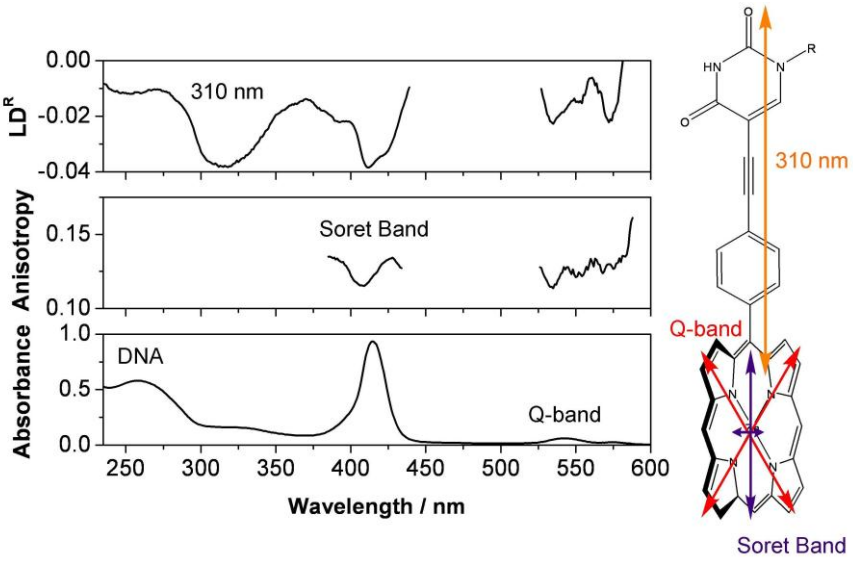


**Figure 3.** Left: Reduced linear dichroism ($LD^R$) spectrum of oligo-ZnP (top), the fluorescence anisotropy spectrum (middle) and the corresponding absorption spectrum (bottom) all in the lipid membrane. No values for $LD^R$ or anisotropy are given where the absorption is so low that these values would be meaningless. The approximate orientations of the ZnP-base-moiety transition moments are indicated in the schematic on the right.

**Linear dichroism and fluorescence anisotropy:** Several important structure details about the relative orientation of oligo-ZnP in the bilayer can be obtained from the $LD^R$ spectrum in Figure 3.

Firstly, the fact that there is a signal at all proves that the structures are indeed anchored to the bilayer as no orientation could have been otherwise achieved since the oligo-ZnP is too short to be oriented in the flow itself. All of the peaks give rise to negative LD signals indicating that the transition moments are at an angle less than 55º to the membrane normal.[17] Dealing firstly with the transition at 310 nm, it seems reasonable to attribute this to a transition moment directed co-linear with the linker moiety and that this is in itself anchored into the membrane at a roughly parallel alignment with the membrane normal. The stiffness of the linker and its long-axis being coplanar with the porphyrin plane suggests that it should go straight down into the membrane. Furthermore, the absolute $LD^R$ value obtained is approximately the same as that achieved for retinoid chromophores which adopt this angle in liposomes of the same composition.[24] This transition moment will therefore be used as the internal reference for the other peaks in the spectrum and it is safe to assume that the orientation parameter, $S$, is the same for all the transitions associated with the ZnP moiety due to its rigidity. Differences in $LD^R$ values are therefore due to the transitions having different angles, $\alpha$, with respect to the orientation axis. The maximum $LD^R$ value of the Soret band is approaching that of the linker moiety but is not a constant value across the absorption peak. This is interesting for two reasons, firstly the deviation from constant $LD^R$ value implies there is an overlap of (two) non-equivalent transitions and the rather high value indicates that the dominant transition is polarized to a greater extent along the long-axis of the group. A doubly-degenerate Soret band would have had an $LD^R$ value half of that of the 310 nm transition and been constant across the peak.[25, 26] This deviation from degeneracy is not unexpected since the porphyrin is not $D_{4h}$ symmetric and it is in fact coupled to the π-system of the linker which therefore might acquire a preferred polarization in that direction. This is seen as a weaker transition polarized in the perpendicular direction but still in the plane of the porphyrin. The Q-band resembles much more what one would expect from a combination of two similar transition moments *i.e.* half the $LD^R$ value of the 310 nm transition. The DNA band centered at 260 nm is relatively weak and has a negative LD. This indicates that the planes of the DNA bases are approximately parallel to the membrane normal but the low value

is best attributed to a lower orientation parameter rather than a specific angle. It should be noted that the porphyrin moiety itself has some absorbance in this region. Since the oligonucleotide is single-stranded its helical structure will be rather loosely defined on the liposome surface and a certain amount of disorder is inevitable, compared to the rigid ZnP moiety. The fact that a signal is seen and is negative does however provide us with the information that the oligonucleotide is lying (roughly) horizontally on the lipid membrane.

It is best to analyze the information obtained from fluorescence anisotropy measurements, in the context of the *LD* results. These complementary methods of determination of transition moments aid greatly in the interpretation of each other. Anisotropy measurements were made both in a glass and in the lipid membrane and the emission was monitored from the Q band at 640 nm. All angles will therefore be related to this transition. The same anisotropy values were obtained in both glass and membrane for the Q-band indicating that this transition is hindered from depolarizing rotations about the linker axis over the lifetime of fluorescence. Excitation of the Q band yields a fundamental anisotropy value of close to 0.1 which is what is expected for an in-plane degenerate transition. This confirms the interpretation of the LD data that the Q band transitions are similar and near degenerate. A similar value close to 0.1 is obtained for the Soret band in the lipid membrane since the emission is from the Q band, in contrast to the $LD^R$ values for the Soret and Q bands being quite different.

**Ligand binding of ZnP:** Binding of the Lewis base 4-*t*-butylpyridine (octanol/buffer partition constant of 300) to the oligo-ZnP in the membrane has been studied using UV-Vis absorption spectroscopy (Figure 4). The octanol-buffer partition constant, $K_{ob}$, is used to approximate the membrane-water equilibrium partitioning. Since the volume ratio between the water and lipid phases is very large, the decrease of substance in the water phase due to uptake into the membrane is neglected in the numerical treatment. Thus, the concentration of the titrant in the lipid phase of the liposomes is calculated as the concentration in the water phase multiplied by $K_{ob}$. Zinc porphyrins are known to coordinate one axial ligand to form a five-coordinated complex.[27-29] The isosbestic point in Figure 4

indicates two spectroscopic species, one being the oligo-ZnP and the other the oligo-ZnP with tBP coordinated to the metal. The peak of the Soret band is shifted from 414 nm for the oligo-ZnP to 422 nm for the tBP coordinated oligo-ZnP as expected from pyridine coordination.[30] Both single-wavelength analysis and Singular Value Decomposition (SVD) were used to calculate the equilibrium constant. In the latter method the entire spectrum is used,[18] which allows highly accurate determination of equilibrium constants without the requirement to titrate all the way to the endpoint. Using the equilibrium $oligo-ZnP+tBP \rightleftharpoons oligo-ZnP-tBP$ as a model reaction and SVD analysis of the entire Soret band (390-440 nm) yields an oligo-ZnP-tBP binding constant of 93 $M^{-1}$. When a single wavelength ($\lambda$ = 413.5 nm) analysis was performed a similar binding constant was achieved. This value is comparable to the values 180 $M^{-1}$ and 1700 $M^{-1}$ for the ligand binding of pyridine to a zinc porphyrin with the same substitution pattern in chloroform and dichloromethane, respectively.[30] This result shows that the ZnP chromophore can be addressed through ligand coordination in the hydrophobic phase of the liposome membrane.

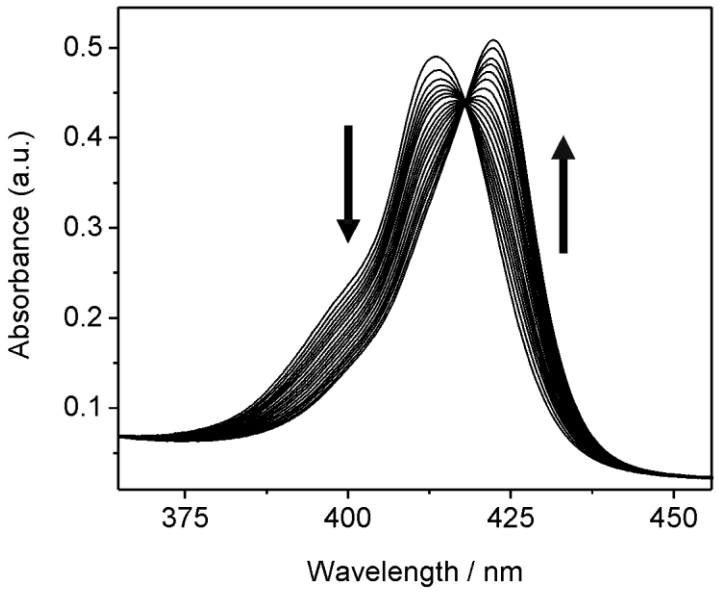


**Figure 4.** Spectrophotometric titration of oligo-ZnP with tBP in the lipid membrane at room temperature. The arrows indicate the decrease of oligo-ZnP absorbance and the increase of oligo-ZnP-

tBP absorbance.

**Quenching of oligo-ZnP fluorescence:** Steady-state and time-resolved fluorescence spectroscopy were used to monitor fluorescence quenching in membranes upon titration with BQ (octanol/buffer partition constant of 2600). Benzoquinones have been proposed to quench zinc porphyrins by a charge transfer mechanism.[31, 32] The driving force for this redox pair is estimated to be around 1 eV which we deemed would be large enough to give substantial electron transfer at donor-acceptor contact.[30, 33] Time-resolved fluorescence spectroscopy shows that the oligo-ZnP exhibits bi-exponential fluorescence decay in the liposome, where the dominating lifetime, ~1.5 ns, is typical for ZnP in less polar solvents and a short lifetime, ~200 ps, that does not seem to be accessible for further quenching. The longer lifetime, however, was substantially quenched upon addition of BQ as shown in Figure 5. Analyzing the decrease in lifetime using the Stern-Volmer equation (Eq. 7) the dynamic quenching constant, $K_d$, was determined to be 2.6 $M^{-1}$. Figure 5 deviate somewhat from the straight line predicted by the Stern-Volemer equation. This deviation might be explained by the partitioning constant, determined at relatively low concentration, being concentration dependent.

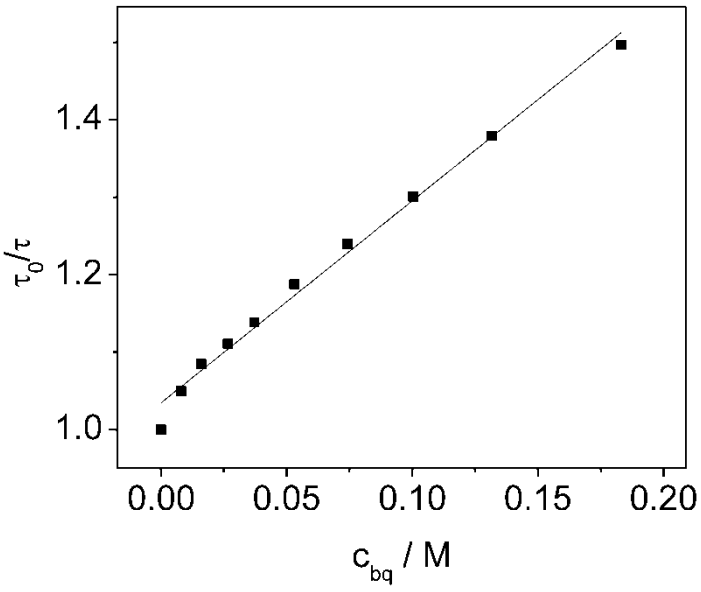


**Figure 5.** Oligo-ZnP fluorescence lifetime as a function of BQ concentration in the lipid membrane at

room temperature. The line is a linear fit using the Stern-Volmer model (eq. 7).

$$\frac{\tau_0}{\tau} = (1 + K_d[Q]) \qquad (7)$$

Fluorescence quenching of the oligo-ZnP was also studied by steady-state spectroscopy (Figure 6). The observed degree of quenching was found to be larger than in the time-resolved experiment. This is explained by a static quenching component. Using the $K_d$ value determined from the time-resolved measurements, the static Stern-Volmer constant, $K_s$, of the quenching was calculated to be 15 $M^{-1}$ using a modified form of the Stern-Volmer equation (Eq. 8). The static Stern-Volmer constant is interpreted as a BQ-oligo-ZnP binding interaction (Eq. 9) that is believed to be due to the weak basic nature of the carbonyl groups. Thus, this binding constant can be compared to the binding constant of *e.g. N,N*-dimethylformamide to a similarly substituted zinc porphyrin in chloroform, 1 $M^{-1}$, and dichloromethane, 8 $M^{-1}$, respectively.[30]

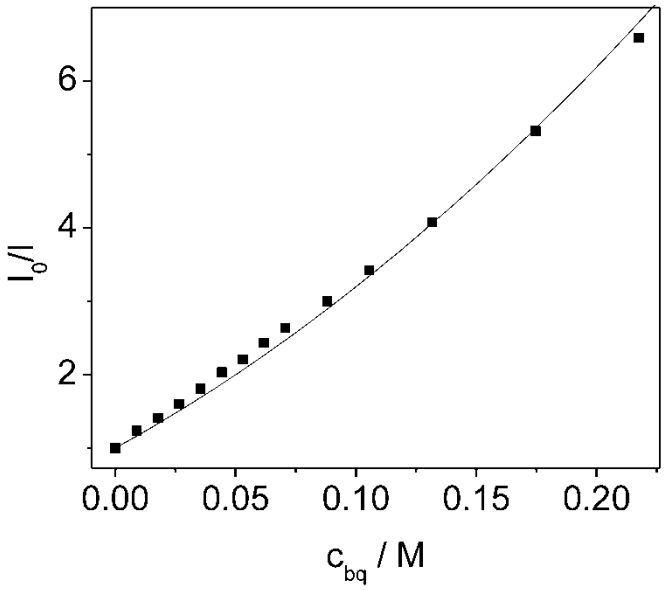


**Figure 6.** Fluorescence emission as a function of BQ concentration in the lipid membrane at room temperature. The line is a fit to a Stern-Volmer model with combined static and dynamic quenching (Eq. 8).

$$\frac{F_0}{F} = (1 + K_d[Q])(1 + K_s[Q]) \qquad (8)$$

$$K_s = \frac{[ZnP - BQ]}{[ZnP][BQ]} \quad (9)$$

For true collisional quenching, the dynamic Stern-Volmer quenching constant is given by $k_q \cdot \tau_0$, where $k_q$ is the bimolecular quenching constant and $\tau_0$ is the lifetime of the fluorophore in absence of quencher. Thus, by dividing the dynamic Stern-Volmer quenching constant with the fluorescence lifetime of the oligo-ZnP (1.5 ns) the bimolecular quenching constant; $k_q = 1.7 \cdot 10^9$ $M^{-1}s^{-1}$, is estimated. The highest possible value for $k_q$ is expected when every fluorophore/quencher encounter results in quenching and denotes the diffusion-controlled bimolecular rate constant, $k_0$. This rate constant can be estimated with the Smoluchowski equation (10):

$$k_0 = \frac{4\pi NR}{1000}(D_q + D_f) \qquad (10)$$

where $N$ is Avogadro's number, $R$ is the collision radius (estimated to be 8 Å), $D_f$ is the fluorophore diffusion constant (set to 0) and $D_q$ is the quencher diffusion constant. The diffusion of a small molecule in a liposome membrane is highly anisotropic. An average was estimated to $3 \cdot 10^{-6}$ $cm^2/s$ given the values for benzene diffusion in membranes.[34] This results in a $k_0$ value of $1.8 \cdot 10^9$ $M^{-1}s^{-1}$, in excellent agreement with the observed rate constant for quenching and shows that the oligo-ZnP chromophores are efficiently quenched in the membrane by BQ.

**Energy transfer between fluorescein and ZnP:** To make use of the supramolecular capacities of DNA the zinc porphyrin strand was hybridized with a strand that either contained a fluorescein at the 3′ or the 5′ end. Efficient singlet excitation energy transfer is expected from fluorescein to the porphyrin because the overlap integral in equation 11 between the fluorescein emission and the oligo-ZnP absorption in the membrane is large (Figure 7). The Förster distance, $R_0$, *i.e.* the donor-acceptor distance at which the energy transfer efficiency is 50%, was determined to be 45 Å using equation 11:

$$R_0 = 0.211\left(\kappa^2 n^{-4} Q_D \int_0^\infty F_D(\lambda)\varepsilon_A(\lambda)\lambda^4 d\lambda\right)^{1/6} \qquad (11)$$

where $\kappa^2$ is an orientation factor assumed to have the value 2/3 (Both the zinc porphyrin and the DNA-linked fluorescein have low but not zero anisotropy),[35] $n$ is the refractive index of the membrane (1.4),[17] $Q_D$ is the donor fluorescence quantum yield in the absence of the acceptor ($Q_D$ = 0.8), $F_D(\lambda)$ is the donor emission spectrum normalized to unity, and $\varepsilon_A(\lambda)$ is the acceptor absorption spectrum. Fluorescein is connected to the DNA 5′ end via an aminohexanol linker and to the 3′-end by a similar 6-carbon linker with a hydroxymethyl side-chain (from 3′-Fluorescein C7 cpg Glen Research). Hybridization of the fluorescein-labeled oligonucleotides with the oligo-ZnP generated two systems which were expected to have different energy transfer efficiencies. The difference in the average fluorescein-zinc-porphyrin distance between the 3′ and 5′ case is 5 base pairs or 17 Å. Time-resolved fluorescence measurements reveals that fluorescein exhibits a bi-exponential lifetime in the fluorescein-zinc-porphyrin system (Table 1). The long lifetime corresponds to fluorescein free in solution (unquenched; $\tau_{uq}$) and the short one is due to energy transfer to the zinc porphyrin ($\tau_q$). Using the quenched lifetime, the energy transfer efficiency for the short distance is 83% and for the long distance 65% (Eq 12) resulting in estimated average donor-acceptor distances (Eq 13), of 35 Å and 41 Å, respectively. Compared to the distances estimated from molecular models (Figure 1) 35 Å is in very good agreement with what is expected for the short distance when the DNA-fluorescein linker is nearly fully stretched whereas 41 Å is somewhat shorter than expected.

$$E = 1 - \frac{\tau_q}{\tau_{uq}} \qquad (12)$$

$$E = \frac{R_0^6}{R_0^6 + r^6} \qquad (13)$$

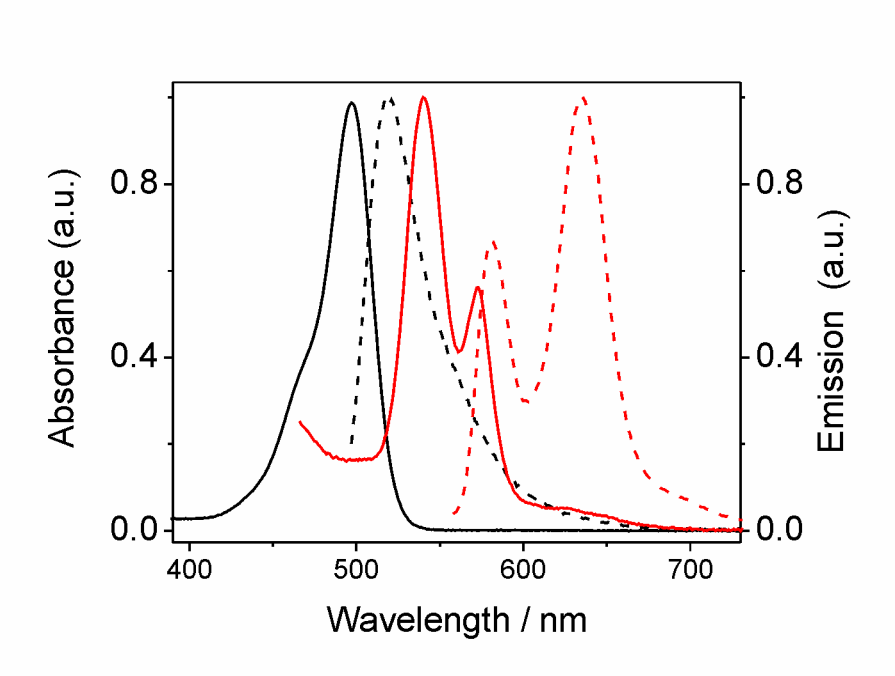


**Figure 7.** Absorption (Q-band) and emission spectra of oligo-ZnP in the lipid membrane (red solid line and red dashed line, respectively) absorption and emission spectra of fluorescein (black solid line and black dashed line, respectively) in phosphate buffer pH 8, all at room temperature.

**Table 1.** Fluorescein fluorescence lifetimes and energy transfer efficiencies in hybridized DNA oligomers at the liposome surface in phosphate buffer pH 8 at room temperature, for the short fluorescein-ZnP distance and for the long fluorescein-ZnP distance.

| | $\tau_1$ ($\alpha_1$) /ns | $\tau_2$ ($\alpha_2$) /ns | $\chi^2_R$ | Efficiency |
|---|---|---|---|---|
| Short distance | 4.2(0.67) | 0.7(0.33) | 1.113 | 0.83 |
| Long distance | 4.3(0.51) | 1.5 (0.49) | 1.087 | 0.65 |

This shows that energy transfer from fluorescein on the complementary strand at the water/membrane interface to the zinc porphyrin in the lipid membrane phase is highly efficient. The fact that a fraction of fluorescein molecules is not transferring energy suggests that the DNA strands are not hybridized completely despite there being an excess of oligo-ZnP strand and that the hybridization procedure was optimized. These experiments were also performed on an 11 base pair long DNA sequence where only a very small fraction of the strands seemed to hybridize. We suggest that the zinc porphyrin hinders the hybridization and the longer the DNA the less pronounced is this effect. This result is in good agreement with earlier work.[11] If the temperature is increased the lifetime corresponding to energy transfer disappears, presumably due to DNA melting. A remarkable effect is that when lowering the temperature again the short lifetime does not come back. The difficulty for the DNA to hybridize on the liposome surface is also confirmed by steady state fluorescence melting curves (Figure 8). After the initial melting the fluorescein emission is approximately independent of temperature. This suggests that the DNA melting is not reversible when on the liposome surface. Thus, there cannot be any oligo-ZnP free in solution, but all oligo-ZnP must be bound to the membrane since hybridization can be performed in absence of liposomes. The reason for the inability to hybridize on the liposome surface might be an effect of the short DNA-porphyrin linker that anchors the DNA tightly to the surface and hence prevents the strands from hybridizing due to the steric hindrance close to the membrane surface.

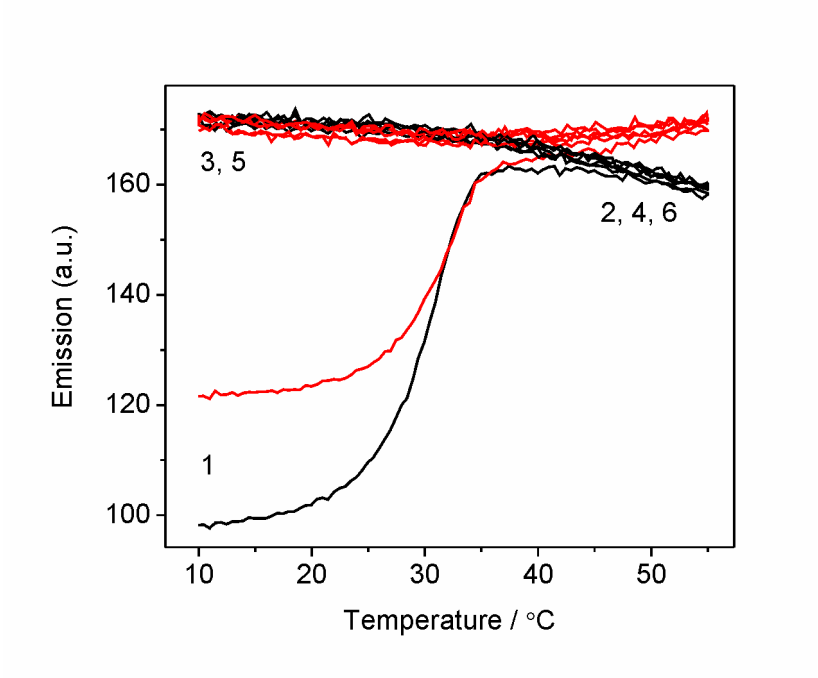


**Figure 8.** Steady state emission melting curve on oligo-ZnP-fluorescein complex with short (black curve) and long (red curve) fluorescein-porphyrin distance. The double stranded DNA is annealed before addition of liposomes. Temperature increases/decreases are shown by numbers in the indicated order.

**Sequential energy and electron transfer:** To demonstrate sequential energy and electron transfer, the fluorescein strand yielding the short fluorescein-porphyrin distance was used. The experiment is in principle quite simple; excite the fluorescein antenna and monitor quenching of the sensitized ZnP emission. However, as was observed in the energy transfer experiments the yield of double-strand after hybridization is only about 50%. This relatively small double-strand yield complicates the evaluation of the sequential energy/electron transfer experiments, since the zinc porphyrin emission is overlapped with the emission from unhybridized fluorescein strands that have a fluorescence quantum yield about two orders of magnitude larger than the zinc porphyrin. However, most of the unwanted emission from fluorescein can be removed by adding a quencher to the solution of the pre-assembled DNA/liposome complex. To this end, a complementary strand containing a 5' BHQ-1$^{TM}$ (Black Hole Quencher$^{TM}$) modification that binds to the free fluorescein modified single strands in solution but not to those on the

liposome will substantially reduce the background fluorescein emission. In fact, this scavenger strand quenches about 95% of the emission from the non-liposome attached fluorescein single-strands (data not shown). As can be seen in Figure 9 the emission of the ZnP decreases with increasing BQ concentration in a manner similar to what was observed upon direct excitation of the porphyrin moiety. It is interesting to compare the amount of quenching in Figure 9 with the case where the porphyrin is directly excited (cf. Figure 6). The amount of ZnP quenching is of a similar magnitude, thus, showing that the amount of electron transfer from ZnP to BQ is independent of whether the porphyrin or the fluorescein antenna is excited. To show that the main part of the porphyrin excitation energy is transferred from fluorescein and not by direct excitation of the porphyrin, and thus, that we have sequential energy and electron transfer in the "supramolecular complex", the emission of single-stranded oligo-ZnP at the same oligo-ZnP concentration as above but in the absence of the fluorescein labeled strand, was monitored as a comparison. As can be seen in Figure 9, about 90% of the unquenched porphyrin emission stems from energy transfer and this agrees very well with the expected amount considering the relative absorption probabilities.[36]

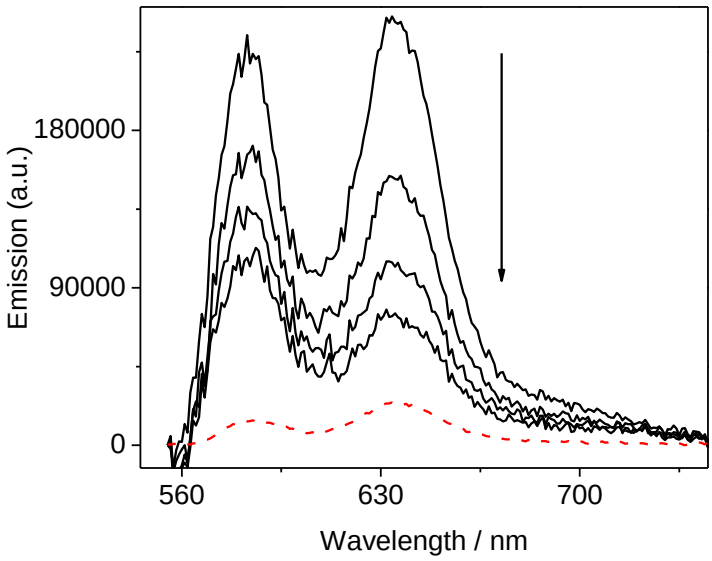


**Figure 9.** Steady state emission spectra of oligo-ZnP-fluorescein complex (black lines) at various BQ

concentrations (0, 49, 97 and 145 mM; Arrow indicates increased amount of BQ). An emission spectrum of fluorescein has been subtracted from the spectra. The low energy peak was used in the analysis of the BQ quenching due to a smaller fluorescein emission overlap and thereby a smaller distortion. The red dashed line shows a steady state emission spectrum of oligo-ZnP monitored at the same oligo-ZnP concentration. All emission spectra were excited at 495 nm (fluorescein absorption maximum) and measured in presence of liposomes and the BHQ modified complementary strands at 10°C (see text).

**Conclusion**

The results above establish some important points in relation to this novel supramolecular energy/electron transfer system. A 14-mer oligonucleotide can be anchored to a large unilamellar lipid vesicle in a defined manner. The anchor itself is multifunctional, being a redox center, an energy acceptor and a ligand binding site. Embedding the chromophore in the bilayer allows transfer of information from the aqueous to the liquid crystalline phase. This result is not merely confirmed by the polarized spectroscopy but rather we can say that the adopted geometry of the entire supramolecular system is resolved. The structure is reasonably well defined with the chromophores firmly anchored in the membrane and their electronic transition moments at fixed angles. Moreover, linear dichroism indicates that the DNA strand itself lies roughly horizontally at the interface. The addressing of the porphyrin with a Lewis base, tBP, in the membrane is demonstrated, as is energy transfer from an antenna (fluorescein) in the water phase to the reaction centre (ZnP) in the lipid membrane and the subsequent electron transfer from ZnP to BQ.

A number of future developments are planned. Since DNA hybridization at the liposome surface is difficult, optimization of the linker length to increase duplex stability and facilitate duplex formation is important. The construction of a functionalized DNA network, similar to what we have reported before,[12, 13] will enable the assembly of a multi-component two dimensional antenna, either consisting

of covalently linked or physically bound (intercalated) antenna fluorophores. Eventually, the utilization of the reduced species inside the membrane should be possible with chemical trapping.

**Acknowledgement**

This research is funded by the European Commission's Sixth Framework Programme (Project reference AMNA, Contract No. 013575).

**Supporting information available**

$^{1}H$, $^{13}C$ NMR of **2**, MALDI-TOF of a test sequence with 12 dT where one dT is substituted with the porphyrin-dT. This material is available free of charge via the Internet at http://pubs.acs.org.

**References**

(1) Huynh, M. H. V.; Dattelbaum, D. M.; Meyer, T. J. *Coord. Chem. Rev.* **2005**, *249*, 457-483.
(2) Sun, L. C.; Hammarström, L.; Åkermark, B.; Styring, S. *Chem. Soc. Rev.* **2001**, *30*, 36-49.
(3) Gust, D.; Moore, T. A.; Moore, A. L. *Acc. Chem. Res.* **2001**, *34*, 40-48.
(4) Erkan, Y.; Czolkos, I.; Jesorka, A.; Wilhelmsson, L. M.; Orwar, O. *Langmuir* **2007**, *23*, 5259-5263.
(5) Czolkos, I.; Erkan, Y.; Dommersnes, P.; Jesorka, A.; Orwar, O. *Nano Lett.* **2007**, *7*, 1980-1984.
(6) Banchelli, M.; Berti, D.; Baglioni, P. *Angew. Chem.-Int. Edit.* **2007**, *46*, 3070-3073.
(7) Clapp, P. J.; Armitage, B.; Roosa, P.; Obrien, D. F. *J. Am. Chem. Soc.* **1994**, *116*, 9166-9173.
(8) Ozeki, H.; Kobuke, Y. *Tetrahedron Lett.* **2003**, *44*, 2287-2291.
(9) Yanagimoto, T.; Komatsu, T.; Tsuchida, E. *Inorg. Chim. Acta* **2000**, *305*, 26-31.
(10) Palacios, R. E.; Kodis, G.; Gould, S. L.; de la Garza, L.; Brune, A.; Gust, D.; Moore, T. A.; Moore, A. L. *ChemPhysChem* **2005**, *6*, 2359-2370.
(11) Fendt, L. A.; Bouamaied, I.; Thoni, S.; Amiot, N.; Stulz, E. *J. Am. Chem. Soc.* **2007**, *129*, 15319-15329.
(12) Tumpane, J.; Kumar, R.; Lundberg, E. P.; Sandin, P.; Gale, N.; Nandhakumar, I. S.; Albinsson, B.; Lincoln, P.; Wilhelmsson, L. M.; Brown, T.; Nordén, B. *Nano Lett.* **2007**, *7*, 3832-3839.
(13) Tumpane, J.; Sandin, P.; Kumar, R.; Powers, V. E. C.; Lundberg, E. P.; Gale, N.; Baglioni, P.; Lehn, J. M.; Albinsson, B.; Lincoln, P.; Wilhelmsson, L. M.; Brown, T.; Nordén, B. *Chem. Phys. Lett.* **2007**, *440*, 125-129.
(14) Pike, A. R.; Ryder, L. C.; Horrocks, B. R.; Clegg, W.; Elsegood, M. R. J.; Connolly, B. A.; Houlton, A. *Chem.-Eur. J.* **2002**, *8*, 2891-2899.
(15) Kajanus, J.; van Berlekom, S. B.; Albinsson, B.; Mårtensson, J. *Synthesis* **1999**, 1155-1162.
(16) Dawson, R. M. C.; Elliot, D. C.; Elliot, W. H.; Jones, K. M. *Data for biochemical*

*research*; Oxford University Press: New York, 1986.
(17) Ardhammar, M.; Lincoln, P.; Nordén, B. *Proc. Natl. Acad. Sci.* **2002**, *99*, 15313-15317.
(18) Kubista, M.; Sjöback, R.; Albinsson, B. *Anal. Chem.* **1993**, *65*, 994-998.
(19) Weber, G.; Teale, F. W. J. *Trans. Faraday Soc.* **1957**, *53*, 646-655.
(20) Ljungdahl, T.; Pettersson, K.; Albinsson, B.; Mårtensson, J. *J. Org. Chem.* **2006**, *71*, 1677-1687.
(21) Anderson, H. L.; Sanders, J. K. M. *J. Chem. Soc. Chem. Commun.* **1989**, 1714-1715.
(22) Bouamaied, I.; Stulz, E. *Synlett* **2004**, 1579-1583.
(23) Fendt, L. A.; Bouamaied, I.; Thoni, S.; Amiot, N.; Stulz, E. *J. Am. Chem. Soc.* **2007**, *129*, 15319-15329.
(24) Svensson, F. R.; Lincoln, P.; Nordén, B.; Esbjörner, E. K. *J. Phys. Chem. B* **2007**, *111*, 10839-10848.
(25) Kim, J. O.; Lee, A.; Jin, B.; Park, T.; Song, R.; Kim, S. K. *Biopys. Chem.* **2004**, *111*, 63-71.
(26) Härd, T.; Nordén, B. *Biopolymers* **1986**, *25*, 1209-1228.
(27) Cole, S. J.; Curthoys, G. C.; Magnusson, E. A.; Phillips, J. N. *Inorg. Chem.* **1972**, *11*, 1024-1028.
(28) Miller, J. R.; Dorough, G. D. *J. Am. Chem. Soc.* **1952**, *74*, 3977-3981.
(29) Vogel, G. C.; Searby, L. A. *Inorg. Chem.* **1973**, *12*, 936-939.
(30) Kilså, K.; Macpherson, A. N.; Gillbro, T.; Mårtensson, J.; Albinsson, B. *Spectrochimica Acta. A* **2001**, *57*, 2213-2227.
(31) Harriman, A.; Porter, G.; Searle, N. *J. Chem. Soc., Faraday Trans. II* **1979**, *75*, 1515-1521.
(32) Yamada, S.; Sato, T.; Kano, K.; Ogawa, T. *Photochem. Photobiol.* **1983**, *37*, 257-262.
(33) Murov, S. L., Carmichael, I. and Hug, G. L. *Handbook of Photochemistry*; Dekker: New York, 1993.
(34) Bassolinoklimas, D.; Alper, H. E.; Stouch, T. R. *Biochemistry* **1993**, *32*, 12624-12637.
(35) Sandin, P.; Lincoln, P.; Albinsson, B., *J. Phys. Chem. C.* **2008,** 112, 13089-13094.
(36) Assuming that half of the fluorescein strands are hybridized, a 50% excess of the porphyrin strand, 83% energy transfer efficiency, and molar absorptivities of 3200 and 75000 $M^{-1}$ $cm^{-1}$ at 495 nm for zinc porphyrin and fluorescein, respectively, the relative amount of excited zinc porphyrin is calculated from: 1.5 μM • 3200 $M^{-1}$ $cm^{-1}$, and the relative amount of excited zinc porphyrin in the assembly from: 1 μM • 3200 $M^{-1}$ $cm^{-1}$ + 0.5 μM • (3200 $M^{-1}$ $cm^{-1}$ + 75000 $M^{-1}$ $cm^{-1}$).

**Toc Graphic**